

## 대변형문제의 컴퓨터 시뮬레이션과 실험

### Physical Experiments and Computer Simulations for Large Deformation Problems

유완석\*·Oleg Dmitrochenko\*\*·박수진\*\*\*·문상혁\*\*\*\*

Wan-Suk Yoo\*, Oleg Dmitrochenko\*\*, Su-Jin Park\*\*\* and Sang-Hyuk Moon\*\*\*\*

**Key Words** : Large deformation, Computer Simulation, Physical Experiments

#### ABSTRACT

In this paper, computer simulations with the absolute nodal coordinate formulation for large deformation problems in flexible multibody dynamics are compared to the real experiments. A high speed camera was employed to capture the deformed shapes of a thin beam, a plate, a rotating chain, and a paper strip. The measured data was used to calculate precise values for stiffness and damping ratio of the objects. Also a rotating strip and a helicoseir problem were formulated for computer simulation, and the computational results are also compared to the experiments.

#### 1. Introduction

The absolute nodal coordinate formulation (ANCF) is a modern finite element technique for modeling large deformation and large displacement problems in flexible multibody dynamics. It produces finite elements that can represent arbitrary large displacements relative to the global frame of reference. The elements employ finite slopes as nodal variables and are generalizations of ordinary finite elements that use infinitesimal slopes. In the ANCF, in contrast with other large deformation formulations, the equations of motion contain a constant mass matrix and a constant vector of generalized gravity forces as well as zero centrifugal and Coriolis inertia forces. Thus, the only nonlinear term in the equations of motion is the vector of elastic forces; it is, however, quite cumbersome to calculate.

In this paper, we suggest a geometrical treatment of the absolute nodal coordinates of a 2D beam. We split them into vectors of nodal displacements and vectors of nodal slopes. The position of an arbitrary point in the beam centerline is then expressed as a linear combination of the nodal vectors with the shape functions used as coefficients. Strain energy, elastic forces and their Jacobian matrices are calculated explicitly using tensor-like relations. We reformulate some known models of elastic forces in our notes and also introduce a couple of new ones. Another subject of the current paper is a rectangular clamped plate undergone large vibration due to a heavy rigid-body weight attached to one of the free edges of the plate. The Kirchhoff model based on ANCF is employed to simulate the plate. We study also the applications of beam finite elements in ANCF such as the helicoseir problem and the rotating strip problem. Helicoseir is a heavy inextensible chain rotating around the vertical axis with only one fixed top point. In spite of its simple physical nature and very interesting behavior, it has a cumbersome mathematical description. Probably, this is the reason why this problem has almost been not mentioned in the literature.

The experimental properties of the helicoseir are as follows. Depending on the initial driving angular velocity of rotation, the chain can take different shapes of relative quasi-equilibrium. The shapes look like one or more half-waves. It is naturally, that a mechanician's mind is very interested in such event and wants to determine its properties like the exact shape of the helicoseir or conditions of its existence.

#### 2. Large deflection of a thin beam

Consider as a finite element the 2D Euler-Bernoulli beam shown in Figure 1. The line running through its center is parameterized by the value  $p = 0 \dots l$ , where  $l$  is the beam's initial length. The vector of the absolute nodal coordinates contains position vectors  $\mathbf{r}_0$ ,  $\mathbf{r}_l$  (of the end points) and the tangent slope vectors  $\boldsymbol{\tau}_0$ ,  $\boldsymbol{\tau}_l$  at these points.

Note that the components of these vectors are not supposed to be small and that tangent vectors may have non-unit lengths. The tangent vectors specify both the declinations and longitudinal deformations of the end points of the element.

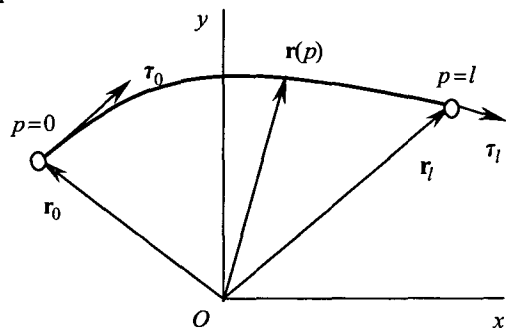


Figure 1. 2D beam finite element

We use the following index notation for the vector of the absolute nodal coordinates of the beam:

$$\mathbf{e} = \begin{Bmatrix} \mathbf{r}_0 \\ \tau_0 \\ \mathbf{r}_l \\ \tau_l \end{Bmatrix} = \begin{Bmatrix} \mathbf{e}_1 \\ \mathbf{e}_2 \\ \mathbf{e}_3 \\ \mathbf{e}_4 \end{Bmatrix}.$$

It can be shown that the position of an arbitrary point on the element is given by the following formula:

$$\mathbf{r}(p) = \begin{bmatrix} s_1 & 0 & s_2 & 0 & s_3 & 0 & s_4 & 0 \\ 0 & s_1 & 0 & s_2 & 0 & s_3 & 0 & s_4 \end{bmatrix} \begin{Bmatrix} r_{0x} \\ r_{0y} \\ \vdots \\ \tau_{lx} \\ \tau_{ly} \end{Bmatrix}$$

with global shape functions defined as follows:

$$s_1 = 1 - 3\xi^2 + 2\xi^3, \quad s_2 = l(\xi - 2\xi^2 + \xi^3), \\ s_3 = 3\xi^2 - 2\xi^3, \quad s_4 = l(\xi^3 - \xi^2), \quad \xi = p/l.$$

For the sake of simplicity, however, we will use slightly different notation to express the same thing:

$$\mathbf{r}(p) = [s_1 \mathbf{I} \quad s_2 \mathbf{I} \quad s_3 \mathbf{I} \quad s_4 \mathbf{I}] \begin{Bmatrix} \mathbf{e}_1 \\ \mathbf{e}_2 \\ \mathbf{e}_3 \\ \mathbf{e}_4 \end{Bmatrix} = \sum_{k=1}^4 s_k \mathbf{e}_k,$$

$\mathbf{I}$  represents the  $2 \times 2$  identity matrix. The equations of motion of the beam element can be obtained from the following Lagrange equations

$$\frac{d}{dt} \left( \frac{\partial T}{\partial \dot{\mathbf{e}}} \right)^T - \left( \frac{\partial T}{\partial \mathbf{e}} \right)^T + \left( \frac{\partial U}{\partial \mathbf{e}} \right)^T = \left( \frac{\delta W}{\delta \mathbf{e}} \right)^T$$

where kinetic energy  $T$  is defined by the equation  $T = \frac{1}{2} \int_0^l \mu \dot{\mathbf{r}}^T \dot{\mathbf{r}} dp$ ,  $U$  represents strain energy, and, finally, the virtual work of external gravity forces is given by  $\delta W = \int_0^l \delta \mathbf{r}^T \mu \mathbf{g} dp$ , where  $\mu$  is the linear density in  $kg/m$ . These equations assume the matrix form:

$$\mathbf{M} \ddot{\mathbf{e}} + \mathbf{Q}^e = \mathbf{Q}^g, \quad (2)$$

where

$$\mathbf{M} = \frac{\mu l}{420} \begin{bmatrix} 156 \mathbf{I} & & & & & & & & \text{sym.} \\ & 22 \mathbf{I} & & 4 l^2 \mathbf{I} & & & & & \\ & & 54 \mathbf{I} & & 13 \mathbf{I} & & 156 \mathbf{I} & & \\ & & & -13 \mathbf{I} & & -3 l^2 \mathbf{I} & & -22 \mathbf{I} & \\ & & & & & & 4 l^2 \mathbf{I} & & \end{bmatrix},$$

$$\mathbf{Q}^e = \begin{Bmatrix} \mathbf{Q}_1^e \\ \mathbf{Q}_2^e \\ \mathbf{Q}_3^e \\ \mathbf{Q}_4^e \end{Bmatrix}, \quad \mathbf{Q}^g = \begin{Bmatrix} \mu \mathbf{g} l/2 \\ \mu \mathbf{g} l^2/12 \\ \mu \mathbf{g} l/2 \\ -\mu \mathbf{g} l^2/12 \end{Bmatrix}.$$

The block elements of the mass matrix  $\mathbf{M}_{ij}$  and the vector of generalized gravity forces  $\mathbf{Q}_i^g$  are defined as:

$$\mathbf{M}_{ij} = \frac{\partial^2 T}{\partial \dot{\mathbf{e}}_i \partial \dot{\mathbf{e}}_j^T} = \underbrace{\mu \int_0^l s_i s_j dp}_{\mathbf{M}_{ij}} \mathbf{I} = M_{ij} \mathbf{I}, \\ \mathbf{Q}_i^g = \frac{\delta W}{\delta \mathbf{e}_i} = \mu \mathbf{g} \int_0^l s_i dp, \quad i, j = 1 \dots 4.$$

The elements of the vector of generalized elastic forces  $\mathbf{Q}_i^e = \partial U / \partial \mathbf{e}_i$  are the most cumbersome ones to deal with due to complexity of the strain energy term  $U$ . The latter decomposes due to the stretching of the beam and the former due to its bending:

$$U = U^\epsilon + U^\kappa = \frac{1}{2} \int_0^l EA \epsilon^2 dp + \frac{1}{2} \int_0^l EI \kappa^2 dp$$

where  $\epsilon$  represents with the longitudinal deformation and  $\kappa$  represents the transverse curvature. The longitudinal  $EA$  and the transverse  $EI$  stiffnesses are assumed to be constant within the beam element. More detail derivation of equations of motion and elastic forces are well explained in reference[1].

To simulate the effects of internal and external friction, we used a linear model of damping forces:

$$\mathbf{Q}^{damp} = \mathbf{D} \dot{\mathbf{e}}$$

In this model, a particular form of proportional Rayleigh damping. It is employed and the system damping matrix assumes the following form:

$$\mathbf{D} = \alpha \mathbf{M} + \beta \mathbf{C} \quad (3)$$

which includes the mass matrix  $\mathbf{M}$  and the stiffness matrix  $\mathbf{C}$  multiplied by the coefficients defined below:

$$\alpha = \frac{2 \omega_1 \omega_2 (\zeta_1 \omega_2 - \zeta_2 \omega_1)}{\omega_2^2 - \omega_1^2}, \\ \beta = \frac{2 (\zeta_2 \omega_2 - \zeta_1 \omega_1)}{\omega_2^2 - \omega_1^2} \quad (4)$$

which themselves depend on the frequencies  $\omega_1$  and  $\omega_2$ , as well as on the damping ratios  $\zeta_1$  and  $\zeta_2$  for the first two modes of the system that appear from the dynamic modal equations:

$$\ddot{x}_i + 2\zeta_i \omega_i \dot{x}_i + \omega_i^2 x_i = 0.$$

The ratios  $\zeta_1$  and  $\zeta_2$  should be calculated from the experimental data.

The most important aspect of any large deformation test is the material. It must be very flexible and elastic, but not plastic. In this test, we have chosen to use a very thin spring-steel beam, which has been heat-treated to increase its strength and durability.

An accelerometer is usually used to measure accelerations and displacements. However, the beam used in this research is too thin to install an accelerometer. Therefore, a high-speed camera is used. The camera also aids in analyzing the displacement of the global deformation.

To compare the efficiency and accuracy of the beam with the ANCF, a stepped cantilever beam shown in Figure 2 was modeled. The stiffer part of the beam was length of 200mm and diameter of 1.4mm, and the thinner part had length of 400mm and diameter of 0.6 mm. For the connection of two parts, a hole, which is 13 mm in depth, was machined by the EDM (electric discharge machine) in the thick beam. The thin beam was inserted into the hole and fixed tightly with glue in order not to be affected by the instability of the connection.

In the hybrid coordinate formulation, the deformation of stiffer part was represented with modal coordinates, and the deformation of thinner part was modeled with ANCF.

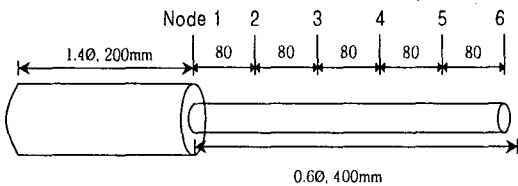


Figure 2. Configuration of a stepped beam

To make the large displacement for a stepped cantilever beam with a base motion, we changed the properties of the beam, which represents the vertical positions of the nodes. As shown in the figure 3, there are just negligible differences in two results.

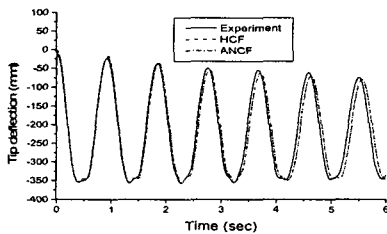


Figure 3. Tip deflection at the tip

### 3. Large deflection of a thin plate

Let us consider a plate element of size  $a \times b \times h$  (length  $\times$  width  $\times$  thickness). Since it is represented only by its middle surface, we will also consider this a thin plate. The surface of the plate is parameterized by the values  $p_1$  and  $p_2$ . Let  $O_1$  be the origin of the configuration space of the element. Then let us imagine a coordinate curve which is parallel to the  $p_1$  axis so that we may define the position  $\mathbf{r}(p_1, p_2)$  of an arbitrary point on the plate relative to the origin  $O$  of the inertial reference frame. Extending of the idea of absolute nodal coordinate formulation to 3D beams gives us the following equation:

$$\mathbf{r}(p_1, p_2) = \begin{bmatrix} \hat{s}_1 \mathbf{I} & \hat{s}_2 \mathbf{I} & \hat{s}_3 \mathbf{I} & \hat{s}_4 \mathbf{I} \end{bmatrix} \begin{Bmatrix} \boldsymbol{\rho}_1 \\ \boldsymbol{\rho}_2 \\ \boldsymbol{\tau}_1 \\ \boldsymbol{\tau}_2 \end{Bmatrix}, \quad (5)$$

where  $\hat{s}_k = s_k(p_1, a)$  are the Hermite shape functions for the  $p_1$ -beam:

$$\begin{aligned} s_1(p, l) &= s_5(l - p, l) = 1 - 3\xi^2 + 2\xi^3, & s_3(p, l) &= 3\xi^2 - 2\xi^3, & \xi &= \frac{p}{l} \\ s_2(p, l) &= -s_4(l - p, l) = l(\xi - 2\xi^2 + \xi^3), & s_4(p, l) &= l(\xi^3 - \xi^2), \end{aligned}$$

and where  $\mathbf{I}$  is the  $3 \times 3$  identity matrix and  $\boldsymbol{\rho}_k$  and  $\boldsymbol{\tau}_k$  are the absolute nodal coordinates of the  $p_1$ -beam (global displacements and slopes of the end points).

The latter vectors  $\boldsymbol{\rho}_k(p_2, b)$  and  $\boldsymbol{\tau}_k(p_2, b)$  depend on the parameter  $p_2$ , which defines the  $p_1$ -beam. For example,  $\boldsymbol{\rho}_1$  is obtained from the bold-faced  $p_2$ -beam shown in Figure 4.

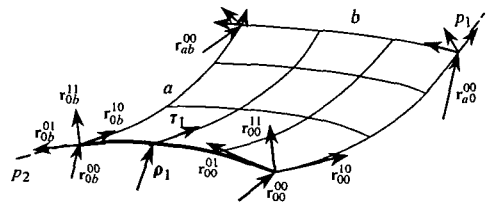


Figure 4. Nodal vectors of a plate FE

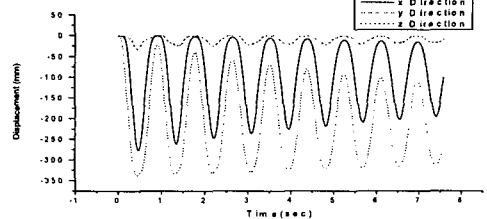


Figure 5. Positions of the tip versus time

The x, y, and z positions of the tip of a 40cm×20.4cm×0.04cm plate with a 260g mass attached to it is shown in Figure 5.

#### 4. Motion of a rotating chain

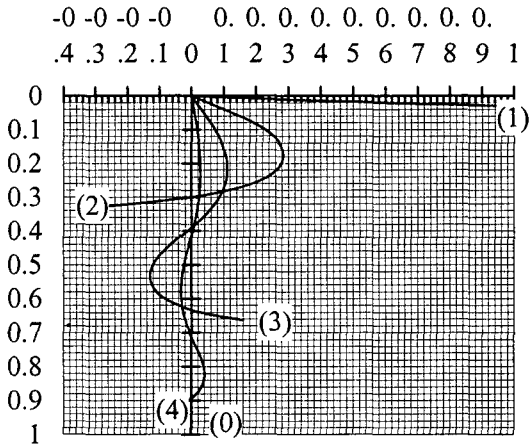


Figure 6. Possible 2D configurations of helicoseir

To start numerical simulation of the helicoseir's motion, one needs to define its initial configuration and velocity. We set the initial configuration corresponding to numerical solution of the two-dimensional model. To describe this part of research we need to repeat some important results obtained in our previous paper [2].

#### 5. A rotating strip

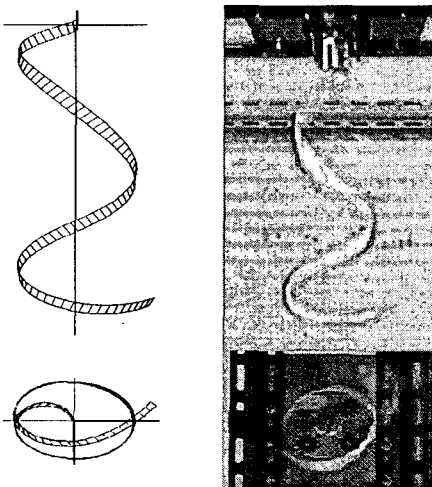


Figure 7. Comparison of a rotating strip

In this chapter, the results of simulations and experiments with thin rotating strip are presented. They do not pretend to be very complete and accurate because

the thorough analysis will require taking into account non-isotropic material properties of the strip. The results are shown here to prove the adequateness of the proposed beam model in principle. The parameters of the model are: length of 0.7 m, width of 15 mm, thickness of 0.1 mm, material density of 750 kg/m<sup>3</sup>, Young modulus of 10<sup>7</sup> Pa, angular velocity of 5 rpm, amount of elements of 16 are used in the simulation. The ratio 'CPU time' / 'model time' is about 450 using a Pentium 4 (CPU 1,7 GHz).

#### 6. Conclusions

We proposed new finite elements of thin three-dimensional beam element and plate element in the absolute nodal coordinate formulation. They have 14 and 48 degrees of freedom, respectively, and incorporate Euler-Bernoulli beam theory and Kirchhof plate theory. The elements allows simulating thin very elastic beams and plates, which gave nice results compared to physical experiments.

We also formulated a rotating strip problem and a helicoseir problem with the ANCF, which are also shown in good agreement with physical experiments.

Thus the authors can conclude that numerical simulation shows a good ability of the proposed elements to represent large displacement and deformation problems in the area of flexible multibody dynamics.

#### Acknowledgement

The authors would like to thank the Ministry of Science and Technology of Korea for financial support in the form of grant (M1-0203-00-0017-02J0000-00910) under the NRL (National Research Laboratory).

#### References

- (1) Wan-Suk Yoo, Su-Jin Park, Joon-Yong Park, and Jeong-Hyun Sohn, "Physical Experiments and Computer Simulations of a Steeped Cantilever Beam with a Hybrid Coordinate Formulation", *Mechanics Based Design of Structures and Machines*, 32(4), 515-532(2004)
- (2) Oleg Dmitrochenko, Wan-Suk Yoo, and Dmitry Pogorelov, "Helicoseir as shape of a rotating chain (II): 3D theory and simulation using ANCF", submitted to *Multibody System Dynamics* (2004)
- (3) Wan-Suk Yoo, Oleg Dmitrochenko, Su-Jin Park, O-Kaung Lim, "A new thin spatial beam element using the absolute nodal coordinates: Application to a rotating strip", submitted to *Mechanics Based Design of Structures and Machines* (2005)